J. Am. Chem. Soc. **1990**, *112*, 3803-3811

A Free Energy Perturbation Study of Solvation in Methanol and Dimethyl Sulfoxide

B. G. Rao and U. C. Singh*

Contribution from the Department of Molecular Biology, Scripps Clinic and Research Foundation, La Jolla, California 92037. Received June 19, 1989

Abstract: Relative differences in free energies of solvation, ΔG, between two different solutes in water, methanol, and dimethyl sulfoxide have been determined by a coordinate coupled free energy perturbation method. The solutes examined in this study are some closed shell ions, tetraalkylammonium ions, normal alkanes, and tetraalkylmethane molecules. The ΔG varies differently in different solvents for the mutation of a solute into another solute. These differences are shown to be resulting from the differences in the solvation processes in different solvents. For closed shell ions, the variation of ΔG shows greater sensitivity to change in the size of an anion in protic solvents than in dipolar aprotic solvent, while it is almost equally affected by the change in the size of a cation in all the three solvents. The structural results of pure liquid and ionic solutions of dimethyl sulfoxide obtained by the molecular dynamics simulations are discussed to rationalize the shape of the ΔG curve for mutations of the closed shell ions in dimethyl sulfoxide. In the case of large tetraalkylammonium ions and alkanes, the variation of ΔG in water is dictated by both the structure of the tight solvent shell around these solutes and the solute–solvent interaction energies. On the other hand, the variation of ΔG for these solutes in methanol and dimethyl sulfoxide are determined mainly by the solute–solvent interaction energies.

Determination of relative free energy differences (ΔG) from computer simulation studies is currently attracting wide attention in view of its potential applications to problems in chemistry and biology.[1] Our recent approach on the free energy perturbation method to calculate the differences in the free energy of hydration of a variety of solute molecules was quite successful.[2] The calculated values were found to be in good agreement with the experimental values. Additionally, we found that the patterns of variation in ΔG with the mutation parameter (λ) are similar for the solutes of the same class and are different for solutes belonging to different classes. These differences are shown to result from differences in the hydration processes of these solutes. For instance, the variation of ΔG with λ for alkylammonium ions is dictated by the large solute–solvent interaction energies. Although the solute–solvent interaction energies are small for alkanes, the pattern of variation of ΔG with λ for these solutes is similar to that of large tetraalkylammonium ions. In both these cases, the variation of ΔG with λ was found to be dictated by the presence of a tight solvent cage around these solutes. However, it is not clear whether this effect is caused by solute–solvent interaction energy or by the intrinsic property of water.[3] We try to address this question in the present study by examining the solvation of different solutes in nonaqueous solvents with use of the same free energy perturbation approach. If the formation of the tight solvent cage around a nonpolar solute is a special property of water, then the variation of ΔG with λ for a given set of nonpolar solutes should be different in nonaqueous solvents as compared to water. Therefore, any difference observed in the variation of ΔG with λ for an apolar solute in water and in a nonaqueous solvent may be attributed to the structural effect of the former. An understanding of the process of solvation in nonaqueous solvents is also of great interest to chemists since these solvents are the principal reaction media in organic chemistry and have important effects on reaction rates.[4,5] Moreover, studies on solvation of apolar, polar, and ionic molecules in different nonaqueous solvents are important for furthering our understanding of the structure and function of biomolecules.[6] Nonaqueous solvation is thought to be quite different and more complicated than aqueous hydration. For instance, it has been possible to treat ionic hydration by simple macroscopic approaches such as Born theory wherein the solvent water is treated as a dielectric continuum.[7] A recent study[8] applied a modified Born model successfully in calculating hydration energies of many ions. Such a treatment of nonaqueous solvation of ions is not possible without adjusting the cavity radius parameter to different values in different solvents. Ionic solvation in different solvents depends on the charge distribution of the solvent molecules and cations may be better solvated in some solvent than anions or vice versa.[9,10] Therefore, a correct description of solvation in nonaqueous solvents should consider explicitly the interaction between the solute and the solvent molecules. However, only a few computer simulation studies on solutions of nonaqueous solvents are reported so far.[11,12]

Table I. Some Properties of Water, MeOH, and DMSO

property	H_2O	MeOH	DMSO
molecular weight (g/mol)	18.015	32.042	78.129
boiling point (°C)	100.0	64.546	189.0
melting point (°C)	0.0	−97.68	18.54
density (g/cm^3)	0.997	0.786	1.0954
isothermal compressibility (10^{-8} Torr^{-1})	6.032	16.640	7.00
dielectric constant	78.3	32.66	46.45
dipole moment (Debye)	1.82	2.87	4.06
viscosity (cP)	0.89	0.55	1.99
surface tension (dynes cm^{-1})	71.81	22.30	42.98
trouton constant (cal deg^{-1} mol^{-1})	26.0	25.0	29.6

We have initiated a free energy perturbation study on the solvation of a variety of solutes in different protic and dipolar aprotic solvents. For the present study, we have chosen two nonaqeuous solvents: a protic solvent, methanol (MeOH), and a dipolar aprotic solvent, dimethyl sulfoxide (DMSO). These two

---

(1) For reviews, see: (a) Beveridge, D. L.; DiCupa, F. M. *Ann. Rev. Biophysics Biophys. Chem.* **1989**, *18*, 431. (b) Van Gunsteren, W. F. *Protein Eng.* **1988**, *2*, 5. (c) Richards, W. G.; King, P. M.; Reynolds, C. A. *Protein Eng.* **1989**, *2*, 319.

(2) Rao, B. G.; Singh, U. C. *J. Am. Chem. Soc.* **1989**, *111*, 3125.

(3) (a) *Water—A Comprehensive Treatise: The Physics and the Physical Chemistry of Water*; Franks, F., Ed.; Plenum Press: New York, 1972; Vol. 1. (b) Lee, B. *Biopolymers* **1985**, *24*, 813.

(4) Abraham, M. H. *Prog. Phys. Org. Chem.* **1974**, *76*, 185.

(5) Parker, A. J. *Chem. Rev.* **1969**, *69*, 1.

(6) (a) Gibson, M. K.; Rashin, A. A.; Fine, R.; Honig, B. *J. Mol. Biol.* **1985**, *183*, 503. (b) Thornton, J. M. *Nature* **1982**, *295*, 13.

(7) For reviews, see: (a) Rossensky, D. R. *Chem. Rev.* **1965**, *65*, 467. (b) Bockris, J. O.'M.; Reddy, A. K. N. *Moern Electrochemistry*; Plenum Press: New York, 1977; Vol. 1. (c) Conway, B. E. *Ionic Hydration in Chemistry and Biophysics*; Elsevier: Amsterdam, The Netherlands, 1981.

(8) Rashin, A. A.; Honig, B. *J. Phys. Chem.* **1985**, *89*, 5588.

(9) Parker, A. J. *Quart. Rev.* **1962**, *16*, 163.

(10) Cox, B. G.; Headwig, G. R.; Parker, A. J.; Walls, D. W. *Aust. J. Chem.* **1974**, *27*, 477.

(11) Chandrasekhar, J.; Jorgensen, W. L. *J. Chem. Phys.* **1982**, *77*, 5080.

(12) Jorgensen, W. L.; Bigot, B.; Chandrasekhar, J. *J. Am. Chem. Soc.* **1982**, *104*, 4584.

0002-7863/90/1512-3803$02.50/0

solvents are not only the most popular solvents in organic chemistry but also have some interesting properties similar to water. Some of these properties[13] are given in Table I. Both MeOH and DMSO are structured to some extent in the liquid state, but no extensive hydrogen-bonding network as in water is observed from the structural studies on these liquids. The liquid structure of MeOH is studied by both X-ray diffraction[14] and theoretical methods.[15,16] Moreover, Monte Carlo simulation studies[11,12] on Na^+ and CH_3O^- ions in MeOH and a RISM analysis[16] of Na^+ and Cl^- in MeOH have been reported. Many structural features of liquid MeOH and its ionic solutions are similar to those of water and its solutions, though there are important differences between them. For instance, the liquid structure of MeOH is made up of small linear chains of MeOH molecules connected by hydrogen bonding though the hydrogen bonding in MeOH is not as extensive as in water. Computer simulation and RISM studies on methanolic solutions of Na^+ show that the coordination number of this ion is the same in both MeOH and water. According to the RISM study, Cl^- ion is coordinated primarily by hydrogen atoms in MeOH. Liquid DMSO or its solutions are not investigated by computer simulation studies. Several proposals were made[17] for the structure of liquid DMSO based on the studies of various physical properties, infrared spectra, and the crystal structure of DMSO. Only recently has X-ray diffraction study on the structure of liquid DMSO been reported.[18] The results of this study suggest that the molecular arrangement in liquid DMSO is similar to that in the crystalline state. However, the structural information from the single average radial distribution function (rdf) obtained in this study is rather limited. We have simulated the structure of pure liquid and ionic solutions of DMSO by molecular dynamics to get a more detailed picture of this liquid. The results of these simulations will also be discussed in this paper.

For the free energy simulations, three different categories of solutes are taken up in the present study. These are (1) small cations and anions, which are differently solvated by different solvents,[5] (2) large alkyl ammonium ions, which have structure-making or structure-breaking effects on water, depending on the size of alkyl groups of these ions,[19] and (3) apolar alkanes which are known to induce unique structural effects in water.[20] The following transformations in MeOH and DMSO are carried out in this study: (1) $Cl^- \rightarrow Br^-$, (2) $Na^+ \rightarrow K^+$, (3) $Me_4N^+ \rightarrow NH_4^+$, (4) $Et_4N^+ \rightarrow Me_4N^+$, (5) $C_2H_6 \rightarrow CH_4$, (6) $Me_4C \rightarrow CH_4$, and (7) $Et_4C \rightarrow Me_4C$. These results are compared with the results reported in our earlier study[2] for these transformations in water. Since the results for the first two transformations in water are not available from our earlier study, these calculations were also carried out in the present study.

Method

The free energy perturbation method[21] is employed in the present study. This method and its implementation into a molecular dynamics program has been described in detail earlier.[22] Briefly, in the free energy perturbation approach, the free energy difference between two states of a system is computed by transforming one state into the other by changing a single coupling parameter in several steps. For instance, the two states, A and B represented by Hamiltonians, $\mathcal{H}_A$ and $\mathcal{H}_B$ are coupled by a dimensionless parameter, λ as

$$\mathcal{H}_\lambda = \lambda\mathcal{H}_A + (1-\lambda)\mathcal{H}_B \qquad 0 \le \lambda \le 1 \tag{1}$$

when $\lambda = 1$, $\mathcal{H}_\lambda = \mathcal{H}_A$ and when $\lambda = 0$, $\mathcal{H}_\lambda = \mathcal{H}_B$. Therefore, the state A can be smoothly transformed to state B by changing the value of λ in small increments, Δλ, such that the system is in equilibrium at all values of λ. At intermediate values of λ, the state is a hypothetical mixture of A and B.

Table II. Charges and Nonbonded Parameters for Halide Ions, Alkali Ions, MeOH, and DMSO

solute	charge	R^* (Å)	ε (kcal)
Cl^-	-1.000	2.4954	0.107
Br^-	-1.000	2.5950	0.090
Na^+	1.000	1.280	0.100
K^+	1.000	1.700	0.100
O(MeOH)	−0.685	1.723	0.170
H(MeOH)	0.400	1.000	0.000
CH_3(MeOH)	0.285	2.119	0.207
O(DMSO)	−0.459	1.650	0.066
S(DMSO)	0.139	2.000	0.202
CH_3(DMSO)	0.160	2.019	0.160

The Gibbs free energy contribution due to the perturbation at every value of λ is given by

$$G_\lambda = -\frac{1}{\beta}\ln\langle\exp(-\beta\mathcal{H}_\lambda)\rangle_0 \tag{2}$$

where $\beta = 1/RT$. The average of $\exp(-\beta\mathcal{H}_\lambda)$ is computed over the unperturbed ensemble of the system. If the perturbation from $\lambda = 1$ to $\lambda = 0$ is carried over N intervals, then the total free energy change equals the sum over all these intervals

$$\Delta G = \sum_{i=1}^{N} G_1(\lambda_i) \tag{3}$$

To circumvent some sampling difficulties during transformation, it is advantageous to decouple ΔG into two parts: an electrostatic part, ΔG_{ele}, and a van der Waals part, ΔG_{vdw}. The ΔG_{ele} represents the free energy change due to the mutation of the partial charges, whereas the ΔG_{vdw} represents the free energy change due to the mutation of the van der Waals parameters such as the radius and the well depth of an atom. This is achieved by transforming the state A to the state B through an intermediate state A′ such that only the partial charges are mutated during the first part of the transformation (A → A′) and the van der Waals parameters are mutated during the second part of the transformation (A′ → B). Further, the technique of coordinate coupling is applied during the mutation of the van der Waals parameters. The details of these methods were described in our earlier paper.[2]

Computational Details

All the calculations were carried out using the AMBER (Version 3.1) program.[23] The details of the protocol used in the computation of the free energy differences using this program were described in detail earlier.[2] A few modifications were made for the present study. Particularly, the EDIT module in the original version of the program, which accepts only "TIP3P water[24] box" as solvent, has been modified to take any assigned solvent box. The solvent boxes of MeOH and DMSO were made as described below.

A solvent box of 216 MeOH molecules was created from the coordinates of the box of 216 TIP3P water molecules by substituting O, H and H positions of water molecules with O, H and CH_3 positions for MeOH. The sides of the box were scaled by an appropriate factor to get the right density for MeOH. This box of MeOH is minimized by conjugate gradient method for 5000 cycles and 100 cycles with SHAKE.[25]

---

[13] *Organic Solvents: Physical Properties and Methods of Purification* (*Techniques of Chemistry*; *Vol. II*); Riddick, J. A., Bunger, W. B., Sakano, T. K., Eds.; John Wiley & Sons: New York, 1986.

[14] (a) Narten, A. H.; Habenschuss, A. *J. Chem. Phys.* **1984**, *80*, 3387. (b) Magini, M.; Paschina, G.; Piccaluga, G. *J. Chem. Phys.* **1982**, *77*, 2051.

[15] (a) Jorgensen, W. L. *J. Am. Chem. Soc.* **1980**, *102*, 543. (b) Jorgensen, W. L. *J. Am. Chem. Soc.* **1981**, *103*, 341.

[16] Hirata, F.; Levy, R. M. *J. Phys. Chem.* **1987**, *91*, 4788.

[17] Szmant, H. H. In *Dimethyl Sulfoxide*; Jacob, S. W., Rosenbau, E. E., Wood, D. C., Eds.; Mercel Dekker: New York, 1981; Chapter 1.

[18] Itoh, S.; Ohtaki, H. *Z. Naturforsch.* **1987**, *42A*, 858.

[19] (a) Kay, R. L.; Evans, D. F. *J. Phys. Chem.* **1966**, *70*, 2325. (b) Kay, R. L.; Vituccio, T.; Zawoyski, C.; Evans, D. F. *J. Phys. Chem.* **1966**, *70*, 2336.

[20] Frank, H. S.; Evans, M. W. *J. Chem. Phys.* **1945**, *13*, 507.

[21] Zwanzig, R. W. *J. Chem. Phys.* **1954**, *22*, 1420.

[22] Singh, U. C.; Brown, F. K.; Bash, P. A.; Kollman, P. A. *J. Am. Chem. Soc.* **1987**, *109*, 1607.

[23] AMBER (Version 3.1) is a fully vectorized version of AMBER (Version 3.0); Singh, U. C.; Weiner, P. K.; Caldwell, J. W.; Kollman, P. A. University of California: San Francisco, 1986. AMBER (Verison 3.1) also includes coordinate coupling and intra/inter decomposition.

[24] Jorgensen, W. L.; Chandrasekhar, J.; Madura, J. D. *J. Chem. Phys.* **1983**, *79*, 926.

[25] SHAKE is an algorithm used to constrain the bond lengths to their equilibrium values druing molecular dynamics. See: Ryckaert, J. P.; Ciccotti, G.; Berendsen, H. J. C. *J. Comput. Phys.* **1977**, *23*, 327.

Table III: The Cutoff Distance and the Number of Solvent Molecules

simulation	solute	ref	solvent	R_c (Å)	no. of MeOH/DMSO
1	Cl^-	Br^-	MeOH	18.0	610
			DMSO	18.0	386
2	Na^+	K^+	MeOH	18.0	610
			DMSO	18.0	382
3	Me_4N^+	NH_4^+	MeOH	12.0	281
			DMSO	18.0	519
4	Et_4N^+	Me_4N^+	MeOH	12.0	336
			DMSO	18.0	578
5	C_2H_6	CH_4	MeOH	12.0	208
			DMSO	18.0	456
6	Me_4C	CH_4	MeOH	12.0	281
			DMSO	18.0	519
7	Et_4C	Me_4C	MeOH	12.0	336
			DMSO	18.0	590

Then it was equilibrated at constant temperature (300 K) and pressure (1 atm) for 20 ps by a molecular dynamics run with a time step of 0.001 ps. A united atom model was used for MeOH, since it was shown by Jorgensen[15] that explicit treatment of the methyl hydrogens was not necessary to obtain a reasonable description of liquid MeOH. Further, MeOH molecules were held rigid by constraining the distances between methyl group and hydroxyl hydrogen. This is in keeping with the formalism[22] used for water. For MeOH, the same nonbonded parameters of Jorgensen[26] were employed in the present study, and these parameters are listed in Table II. Since the studies on the structure and properties of liquid MeOH are already reported by Jorgensen,[15] these calculations are not repeated here. The coordinates from the equilibrated structure of the liquid MeOH box were used for free energy calculations.

The DMSO box was also made by a similar treatment. The O, H and H positions of water were substituted by S, CH_3 and CH_3 of DMSO, and O of DMSO was positioned on the bisecter of the CH_3–S–CH_3 angle, away from the methyl groups. The length of the DMSO box was scaled to get the correct density of DMSO. DMSO molecules were held rigid by constraining the distances between the two methyl groups and oxygen atom. The nonbonded parameters, R and ϵ, for the atoms of DMSO were taken from Allinger and Kao.[27] For the methyl groups of DMSO also, a united atom model was adopted. The bond lengths and angles of DMSO are those determined from microwave spectroscopy by Feder et al.[28] The partial charges for DMSO were obtained by fitting the electrostatic potential around this molecule to a point charge model.[29] The electrostatic potential of the molecule was obtained by the ab initio program QUEST[30] with a 6-31G* basis set.[31] Since ab initio calculation with 6-31G* basis set is known[32] to overestimate partial charges by a factor of 0.87, we scaled these charges by the same factor. This charge model of DMSO gives a dipole moment of 4.30 D. The charges and the nonbonded parameters of DMSO are listed in Table II. The box of 216 DMSO molecules was minimized in two stages as described earlier. The minimized coordinates were used as the starting point for the molecular dynamics simulations of liquid DMSO at constant temperature (300 K) and constant pressure (1 atm) by using SHAKE and periodic boundary conditions. The time step used in these simulations was 0.001 ps, and the coordinates were collected at every 0.1 ps for a time period of 100 ps. The density and the radial distribution functions (rdfs) of liquid DMSO were computed from the coordinates over the last 80 ps. The average density of the simulated DMSO is 1.090 ± 0.010 gm/cc, which is in good agreement with the experimental value of 1.1014 gm/cc. The calculated rdfs are also in good agreement with those determined by X-ray diffraction (see later in Discussion). Therefore, the final coordinates from the molecular dynamics run were used for the simulation of ionic solutions and for the free energy calculations in DMSO. For molecular dynamics simulation of ionic solutions of DMSO, the solute ion was placed at the center of a box containing three cubes of 216 DMSO molecules obtained from the earlier simulation of pure liquid DMSO. The solvent molecules farther than a distance of 18 Å from the solute were discarded. This resulted in a cubic box of 386 DMSO molecules around Cl^- ion and a cubic box of 382 DMSO molecules around Na^+ ion. These two systems were equilibrated for 10 ps, and the coordinates were collected for the next 50 ps for computing rdfs.

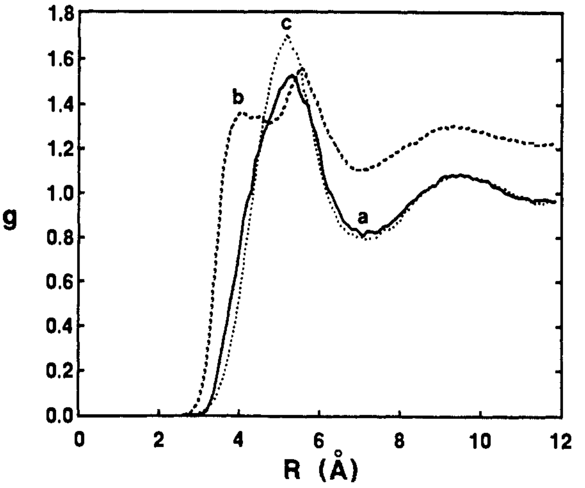

Figure 1. Radial distribution functions of (a) S–S, (b) C–C, and (c) O–O pairs of liquid DMSO.

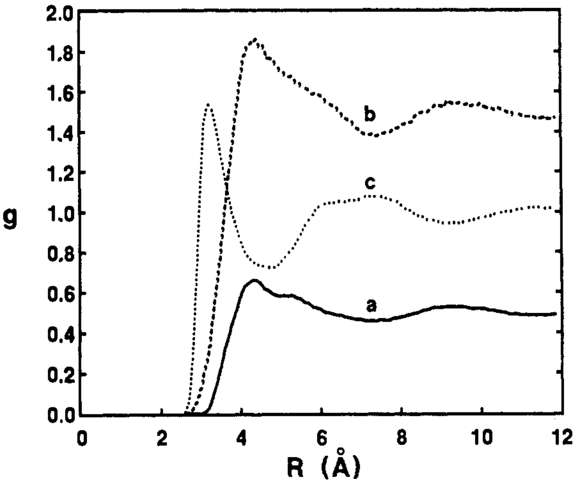

Figure 2. Radial distribution functions of (a) S–C, (b) S–O, and (c) C–O pairs of liquid DMSO.

For the free energy calculations, the force field parameters and the partial charges for alkanes and tetraalkylammonium ions were taken from our earlier paper.[2] The van der Waals parameters, R and ϵ for alkali ions (Na^+ and K^+) and halide ions (Cl^- and Br^-), were taken from Lybrand and Kollman[33] and Lybrand et al.,[34] respectively. These parameters are listed in Table II. These solutes were solvated by MeOH and DMSO as described earlier. In addition, the alkali and halide ions were solvated by TIP3P water. The cutoff distances and the number of the solvent molecules solvating each solute are listed in Table III for all the transformations. Each system was minimized in four stages. First, the solvent around the solute was minimized for 500 cycles with steepest descent method. Second, it was minimized for the next 2000 cycles with conjugate gradient method. Third, the whole system was minimized with conjugate gradient method for another 1000 cycles followed by a minimization of 100 cycles with SHAKE. The system was initially equilibrated for 6.5 ps at constant temperature (300 K) and pressure (1 atm) by using a time step of 0.002 ps. During minimization, equilibration, and the subsequent perturbation runs, periodic boundary conditions were applied only for solute–solvent and solvent–solvent interactions. A constant dielectric of 1 was used for all simulations. For solute–solvent and solvent–solvent nonbonded interactions, cutoff distances of 10 and 12 Å were employed for simulations in MeOH and DMSO, respectively. All solute–solute nonbonded interactions were included. The nonbonded pair list was updated very 100 molecular dynamics steps. For the transformations involving closed shell ions, 101 windows were employed with 0.4 ps equilibration followed by 0.4 ps of data collection at each window. For the molecular solutes, the mutation was achieved in two stages by using

---

(26) Jorgensen, W. L. *J. Am. Chem. Soc.* **1981**, *103*, 335.

(27) Allinger, N. L.; Kao, J. *Tetrahedron* **1976**, *32*, 529.

(28) Feder, W.; Dreizler, H.; Rudolf, H. D.; Typke, V. *Z. Naturforsch.* **1969**, *24A*, 266.

(29) Singh, U. C.; Kollman, P. A. *J. Comput. Chem.* **1984**, *5*, 129.

(30) QUEST (Version 1.0); Singh, U. C.; Kollman, P. A. University of California: San Francisco, 1986. QUEST includes GAUSSIAN80; by Brinkly, J. S.; Frisch, M.; Krishnan, R.; DeFrees, D. J.; Schlegel, H. B.; Whiteside, R.; Fluder, E.; Seeger, R.; Pople, J. A. Carnegie-Mellon University, 1980.

(31) Hariharan, P. C.; Pople, J. A. *Theor. Chim. Acta* **1973**, *28*, 213.

(32) Cox, S. R.; Williams, D. E. *J. Comput. Chem.* **1981**, *2*, 304.

(33) Lybrand, T. P.; Kollman, P. A. *J. Chem. Phys.* **1985**, *83*, 2923.

Table IV. Pair Distances and Coordination Numbers (CN) from Molecular Dynamics (MD) and X-ray Diffraction

	distance (Å)		
pair	MD	X-ray[a]	CN[b]
S–S	5.3	5.25	12 (7.1)
S–C	4.25	4.26	
S–O	4.4	4.05	
C–C	4.1, 5.5	4.26	
C–O	3.2	3.29	3 (4.8)
O–O	5.15	5.12	12 (7.1)
Cl^-–S	4.25–5.35		7 (5.8)
Cl^-–C	3.75		14 (5.7)
Cl^-–O	5.8		
Na^+–S	3.45		5 (3.9)
Na^+–C	4.2–4.7		
Na^+–O	2.15		5 (2.5)

[a] The averaged pair distances from ref 18. [b] The values in parentheses are the cutoff distances used in the integration of the first peaks of different rdfs to get the coordination numbers.

the free energy decoupling method.[2] The partial charges were mutated first by using 21 windows with 1.0 ps of equilibration and 1.0 ps of data collection at each window. The van der Waals parameters were mutated with coordinate coupling over 201 windows with 0.2 ps of equilibration and 0.2 ps of data collection. The time step used during equilibration and data collection was 0.002 ps. Simulations involving closed shell ions were repeated with larger cutoff distance (14 Å) for the solute–solvent and the solvent–solvent nonbonded interactions and larger number of windows to check the dependence of the calculated values on these simulation parameters. The results of the two sets of simulations were found to differ only marginally by about 2–3%.

Results

(a) Radial Distribution Functions. The radial distribution functions (rdfs) for all the intermolecular pairs of atoms of DMSO are given in Figures 1 and 2. As the intramolecular bond distances were constrained, the rdfs for these pairs were not computed. The rdfs show two peaks for S–S, O–O and C–O pairs. The C–C pair distribution shows a split first peak. The peaks of S–O and S–C pairs are not well defined. The rdfs for S–S and O–O pairs are similar and the same is true for the rdfs of S–O and S–C pairs. The pair distances obtained from the positions of the first maxima in these rdfs are given in Table IV along with the values obtained from the X-ray diffraction study.[18] For some peaks, it was possible to obtain the coordination numbers from the areas under those peaks. These coordination numbers are also given in Table IV. The S–S and O–O peaks, respectively, at 5.3 and 5.15 Å integrate to approximately 12 suggesting that a DMSO molecule is coordinated by about 12 other molecules in the liquid state. The methyl groups of DMSO are coordinated by oxygens of three DMSO molecules at a distance of 3.2 Å. The S–C and S–O pairs peak at 4.25 and 4.4 Å, respectively, and then decrease almost continuously after the first peak. This suggests that the S–O and S–C intermolecular correlations are weak. The C–C pairs have peaks at 4.1 and 5.5 Å due to the rigid positioning of two methyl groups on a single molecule. The rdfs for Cl^- and Na^+ ions with the atoms of DMSO are given in Figures 3 and 4, respectively. The rdfs of the Cl^-–C and Cl^-–O pairs show well-defined peaks, whereas a broad peak with several small maxima is observed in the rdf of the Cl^-–S pair. The Cl^-–C peak at 3.75 Å integrates to a coordination number of about 14. The Cl^-–O peak at 5.8 Å and the Cl^-–S peak integrate to a coordination number of about 7, suggesting that about seven DMSO molecules coordinate the Cl^- ion. The rdfs for the pairs of Na^+ ion with the atoms of DMSO show intense peaks. Particularly, the first peak in the rdf of Na^+–O pair at 2.15 Å is very sharp and intense. This peak integrates exactly to a coordination number of 5, and the coordination number of Na^+–S pair positioned at 3.45 Å is also equal to 5. Therefore, both the Na^+–O and Na^+–S rdfs indicate that the Na^+ ion is coordinated by five DMSO molecules. The Na^+–C pair shows a broad peak spreading from 4.2 to 4.7 Å. The rdfs of the intermolecular pairs of solvent atoms obtained from the simulations of the two solutions were found to be exactly similar to those of the pure liquid.

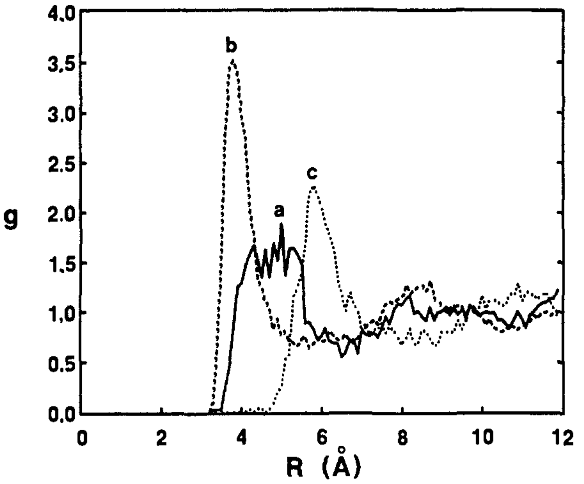

Figure 3. Radial distribution functions of (a) Cl^-–S, (b) Cl^-–C, and (c) Cl^-–O pairs of liquid DMSO solution of Cl^-.

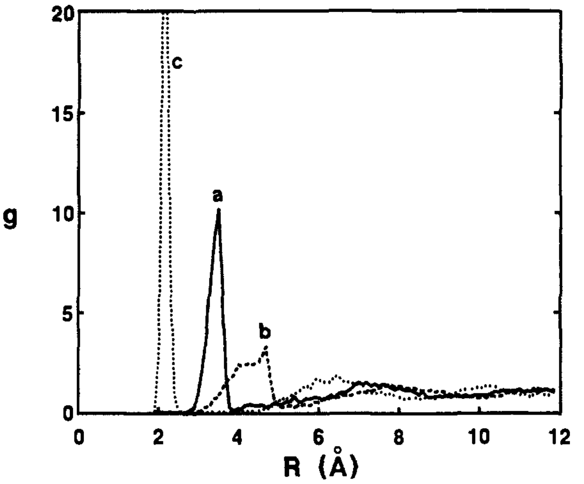

Figure 4. Radial distribution functions of (a) Na^+–S, (b) Na^+–C, and (c) Na^+–O pairs of liquid DMSO solution of Na^+.

(b) Free Energy Differences. The calculated free energy differences and the experimental values from the literature for all the transformations are summarized in Table V. For each transformation, the electrostatic part, ΔG_{ele}, the van der Waals part calculated with coordinate coupling, $\Delta G_{vdw/cc}$, and their sum are listed. The data for molecular solutes in water are taken from our earlier paper.[2] For all cases, the dominant contribution to the total free energy difference comes from the $\Delta G_{vdw/cc}$ term. The ΔG_{ele} values are small in all cases and are almost negligible for neutral alkanes. The experimental values of free energy of solvation of different solutes in MeOH and DMSO were obtained by adding the values of free energy of transfer, ΔG_{tr} (water → solvent), of the solutes to the corresponding values of free energy of hydration.[35] Unfortunately, the experimental ΔG_{tr} values reported for some solutes may not be very accurate since these were determined by using extrathermodynamic assumptions, and different groups employed different sets of assumptions in deriving the ΔG_{tr} values. This makes the assessment of the accuracy of the calculated values difficult. The experimental values listed in Table V were obtained from thd ΔG_{tr} values recommended as best

---

(34) Lybrand, T. P.; Indira, G.; McCammon, J. A. *J. Am. Chem. Soc.* **1985**, *107*, 7793.

(35) Free energy of hydration values for alkali ions and halide ions are taken from the following: (a) Friedman, H. L.; Krishnan, C. V. In *Water—A Comprehensive Treatise*; Franks, F., Ed.; Plenum Press: New York, 1973; Vol. 3, p 1. The values for ammonium ion are taken from the following: (b) Aue, D. H.; Webb, H. M.; Bowers, M. T. *J. Am. Chem. Soc.* **1976**, *21*, 318. The values for tetraalkylammonium ions are taken from the following: (c) Abraham, M. H.; Liszi, J. *J. Chem. Soc., Faraday Trans. 1* **1978**, *74*, 1604. The values for alkanes are from ref 37.

Table V. Calculated and Experimental Free Energy Changes[a]

solute	ref	solvent	ΔG_{ele}	$\Delta G_{vdw/cc}$	total	expt
Cl^-	Br^-	H_2O		3.23 ± 0.05	3.23 ± 0.05	3.3
		MeOH		3.03 ± 0.05	3.03 ± 0.05	3.8
		DMSO		1.26 ± 0.04	1.26 ± 0.04	0.2
Na^+	K^+	H_2O		20.09 ± 0.07	20.09 ± 0.07	17.5
		MeOH		20.13 ± 0.08	20.13 ± 0.08	17.8
		DMSO		20.17 ± 0.09	20.17 ± 0.09	17.6
Me_4N^+	NH_4^+	H_2O	-0.65 ± 0.00	-29.17 ± 0.52	-29.82 ± 0.52	-31.7
		MeOH	-0.59 ± 0.00	-29.05 ± 0.28	-29.64 ± 0.28	-31.9
		DMSO	-0.54 ± 0.03	-29.20 ± 0.60	-29.74 ± 0.63	
Et_4N^+	Me_4N^+	H_2O	-0.64 ± 0.01	-6.10 ± 0.25	-6.74 ± 0.26	-7.0
		MeOH	-0.79 ± 0.00	-4.43 ± 0.34	-5.22 ± 0.34	-5.8
		DMSO	-0.53 ± 0.00	-4.50 ± 0.32	-5.03 ± 0.32	-5.3
C_2H_6	CH_4	H_2O	-0.09 ± 0.01	-0.33 ± 0.02	-0.42 ± 0.03	0.2
		MeOH	-0.06 ± 0.00	0.37 ± 0.01	0.31 ± 0.01	0.9
		DMSO	-0.03 ± 0.02	0.18 ± 0.04	0.15 ± 0.06	1.1
Me_4C	CH_4	H_2O	-0.05 ± 0.01	-0.81 ± 0.07	-0.86 ± 0.08	-0.5
		MeOH	0.01 ± 0.00	1.89 ± 0.01	1.90 ± 0.02	1.9
		DMSO	-0.09 ± 0.01	1.38 ± 0.03	1.29 ± 0.04	
Et_4C	Me_4C	H_2O	0.05 ± 0.00	0.35 ± 0.01	0.40 ± 0.01	0.2
		MeOH	0.05 ± 0.00	1.66 ± 0.04	1.71 ± 0.04	2.5
		DMSO	0.01 ± 0.00	1.84 ± 0.02	1.85 ± 0.02	

[a] All values are in kcal/mol.

Table VI. Interaction Energies of Solutes in Water, MeOH, and DMSO[a]

solute	H_2O	MeOH	DMSO
Cl^-	-134.3 ± 5.7	-100.2 ± 8.1	-79.0 ± 7.6
Br^-	-132.2 ± 5.0	-112.4 ± 6.6	-87.8 ± 4.2
Na^+	-195.7 ± 8.8	-179.9 ± 3.5	-194.5 ± 6.6
K^+	-155.6 ± 7.5	-164.7 ± 6.0	-169.1 ± 4.4
NH_4^+	-138.5 ± 6.4	-144.0 ± 4.5	-161.2 ± 3.4
Me_4N^+	-100.2 ± 7.0	-93.4 ± 3.3	-102.0 ± 6.6
Et_4N^+	-96.7 ± 5.9	-91.2 ± 4.4	-97.5 ± 6.9
CH_4	-2.8 ± 0.6	-2.3 ± 0.2	-2.7 ± 0.3
C_2H_6	-4.9 ± 0.7	-2.9 ± 0.5	-4.1 ± 0.7
Me_4C	-8.4 ± 0.8	-5.8 ± 0.3	-8.2 ± 1.0
Et_4C	-13.2 ± 0.9	-6.7 ± 0.9	-12.7 ± 1.0

[a] All values are in kcal/mol.

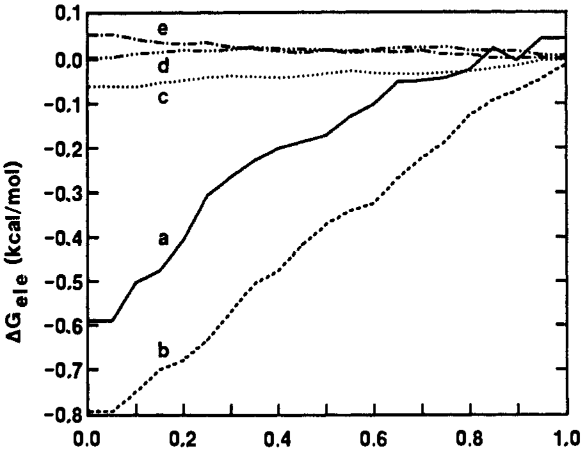

Figure 5. Variation of ΔG_{ele} with λ for transformations in MeOH: (a) $Me_4N^+ \rightarrow NH_4^+$, (b) $Et_4N^+ \rightarrow Me_4N^+$, (c) $C_2H_6 \rightarrow CH_4$, (d) $Me_4C \rightarrow CH_4$, and (e) $Et_4C \rightarrow Me_4C$.

by Marcus[36] for ionic solutes, and the values for alkanes are from Abraham.[37] The calculated solute–solvent interaction energies for the solutes in the three solvents are given in Table VI.

The variations of ΔG_{ele} with λ for various transformations in MeOH and DMSO are shown in Figures 5 and 6, respectively. For neutral alkanes, ΔG_{ele} varies little with λ. The values of ΔG_{ele} for the transformations of these solutes are smaller than 0.1 kcal/mol. For positively charged alkylammonium ions, however, ΔG_{ele} decreases with λ. For the $Me_4N^+ \rightarrow NH_4^+$ transformation, it decreases to -0.59 kcal/mol in MeOH and -0.54 kcal/mol in DMSO, and for the $Et_4N^+ \rightarrow Me_4N^+$ transformation, it decreases to -0.79 kcal/mol in MeOH and -0.53 kcal/mol in DMSO. These values are also small compared to the corresponding $\Delta G_{vdw/cc}$

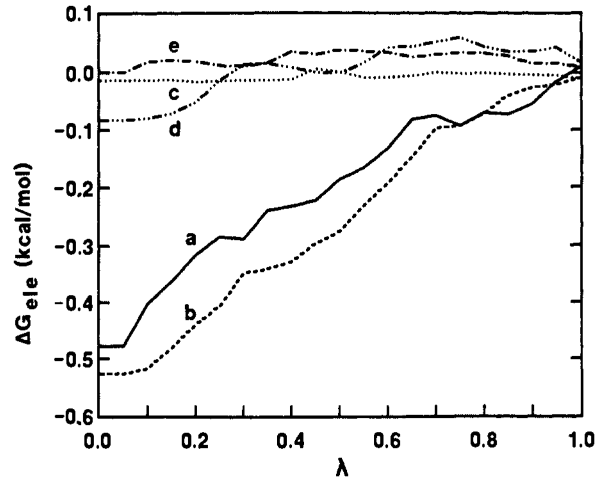

Figure 6. Variation of ΔG_{ele} with λ for transformations in DMSO: (a) $Me_4N^+ \rightarrow NH_4^+$, (b) $Et_4N^+ \rightarrow Me_4N^+$, (c) $C_2H_6 \rightarrow CH_4$, (d) $Me_4C \rightarrow CH_4$, and (e) $Et_4C \rightarrow Me_4C$.

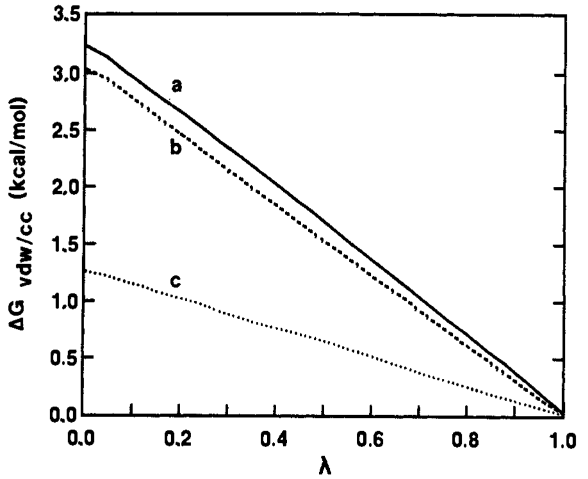

Figure 7. Variation of $\Delta G_{vdw/cc}$ with λ for $Cl^- \rightarrow Br^-$ transformation in (a) water, (b) MeOH, and (c) DMSO.

---

(36) Marcus, Y. *Pure Appl. Chem.* **1983**, *55*, 977.
(37) Abraham, M. H. *J. Am. Chem. Soc.* **1982**, *104*, 2085.

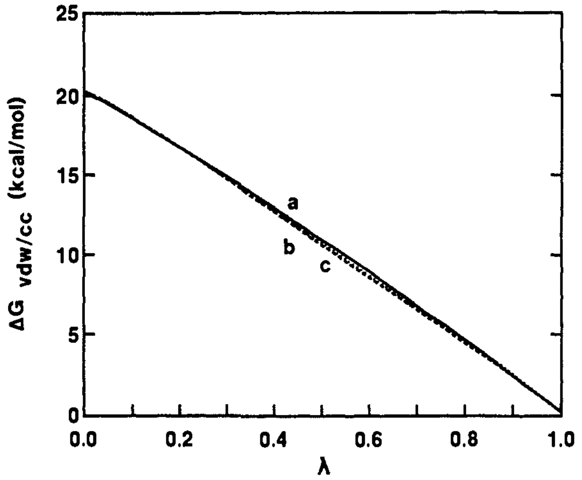

Figure 8. Variation of $\Delta G_{vdw/cc}$ with λ for $Na^+ \rightarrow K^+$ transformation in (a) water, (b) MeOH, and (c) DMSO.

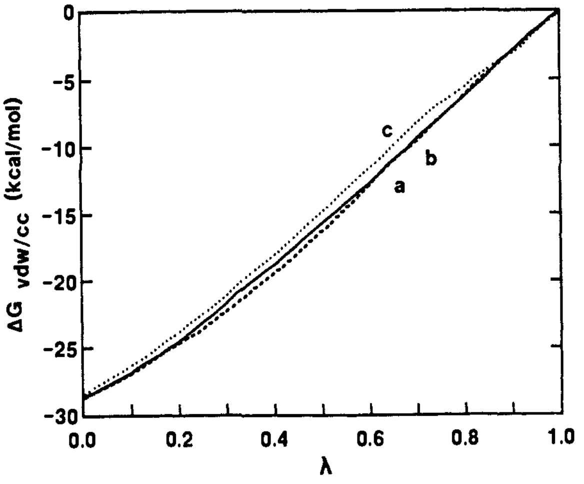

Figure 9. Variation of $\Delta G_{vdw/cc}$ with λ for $Me_4N^+ \rightarrow NH_4^+$ transformation in (a) water, (b) MeOH, and (c) DMSO.

values for the same transformations.

The variation of $\Delta G_{vdw/cc}$ with λ for the transformation of $Cl^- \rightarrow Br^-$ in water, MeOH, and DMSO is given in Figure 7. In all the three solvents, $\Delta G_{vdw/cc}$ increases linearly with λ. The increase is highest in water, in which case $\Delta G_{vdw/cc}$ reaches a value of 3.23 kcal/mol. In MeOH, $\Delta G_{vdw/cc}$ increases to 3.03 kcal/mol, a value very close to that in water. However, the rate of increase of $\Delta G_{vdw/cc}$ in DMSO is not as high as in water or MeOH, and the final value is only 1.26 kcal/mol. The variation of $\Delta G_{vdw/cc}$ with λ for transformation of $Na^+ \rightarrow K^+$ in water, MeOH, and DMSO is given in Figure 8. In this case also, $\Delta G_{vdw/cc}$ increases linearly with λ and the rate of increase of $\Delta G_{vdw/cc}$ is almost equal for all the three solvents. The final $\Delta G_{vdw/cc}$ values are 20.09, 20.22, and 20.17 kcal/mol, respectively, in water, MeOH, and DMSO.

For transformation of $Me_4N^+ \rightarrow NH_4^+$ in water, MeOH, and DMSO, the variation of $\Delta G_{vdw/cc}$ with λ is given in Figure 9. The $\Delta G_{vdw/cc}$ decreases linearly, and the rate of decrease is almost the same for all the three solvents. The final $\Delta G_{vdw/cc}$ values are −29.17, −29.05, and −29.20 kcal/mol in water, MeOH, and DMSO, respectively, and the corresponding total free energy differences are −29.82, −29.64, and −29.74 kcal/mol. The variation of $\Delta G_{vdw/cc}$ with λ for transformation of $Et_4N^+ \rightarrow Me_4N^+$ in water, MeOH, and DMSO is given in Figure 10. The $\Delta G_{vdw/cc}$ initially decreases sharply than in the later part of the transformation. The pattern is almost same in all the solvents. The final $\Delta G_{vdw/cc}$ values in MeOH and DMSO are −4.43 and −4.50 kcal/mol, respectively. Both these values are lower than the corresponding value in water (−6.10 kcal/mol). The total free energy changes are −5.22 and −5.03 kcal/mol in MeOH and DMSO, respectively.

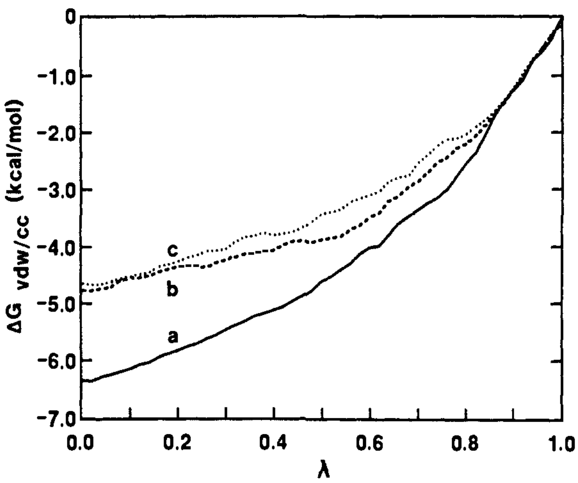

Figure 10. Variation of $\Delta G_{vdw/cc}$ with λ for $Et_4N^+ \rightarrow Me_4N^+$ transformation in (a) water, (b) MeOH, and (c) DMSO.

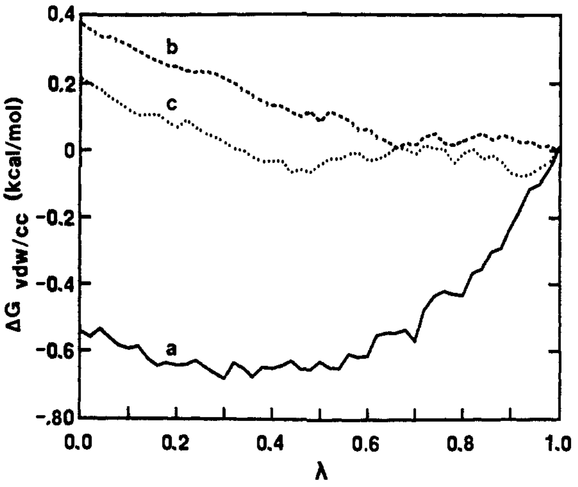

Figure 11. Variation of $\Delta G_{vdw/cc}$ with λ for $C_2H_6 \rightarrow CH_4$ transformation in (a) water, (b) MeOH, and (c) DMSO.

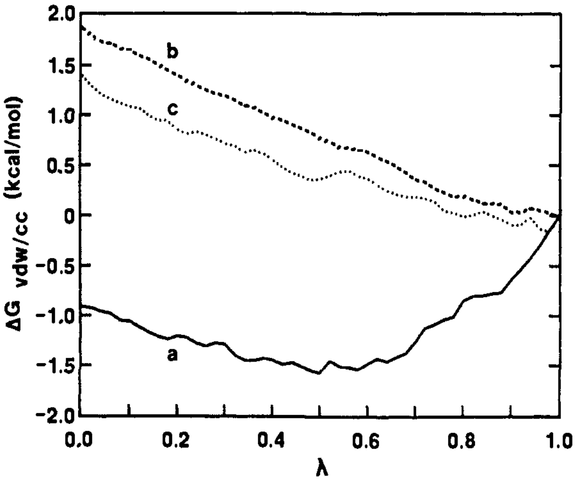

Figure 12. Variation of $\Delta G_{vdw/cc}$ with λ for $Me_4C \rightarrow CH_4$ transformation in (a) water, (b) MeOH, and (c) DMSO.

The variation of $\Delta G_{vdw/cc}$ with λ for transformation of $C_2H_6 \rightarrow CH_4$ in water, MeOH, and DMSO is given in Figure 11. The $\Delta G_{vdw/cc}$ increases almost linearly in MeOH, whereas it shows two small dips in DMSO and increases after the second dip almost parallel to the curve corresponding to MeOH. In contrast, the curve for water shows a broad dip. The final $\Delta G_{vdw/cc}$ values are 0.37 and 0.18 kcal/mol in MeOH and DMSO, respectively, and the total free energy differences are 0.31 and 0.15 kcal/mol. For $Me_4C \rightarrow CH_4$ transformation, the variation of $\Delta G_{vdw/cc}$ versus

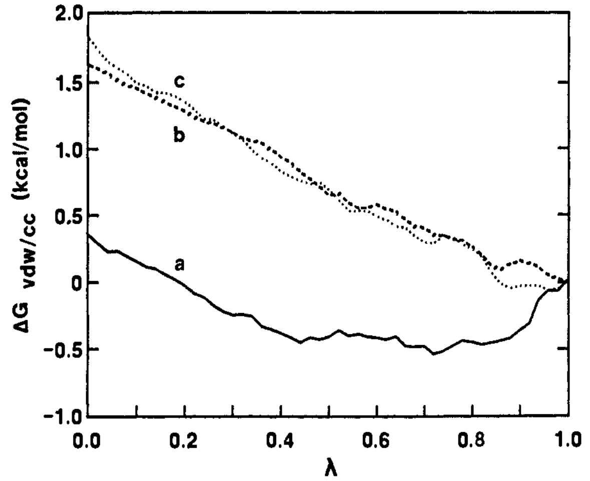

Figure 13. Variation of $\Delta G_{vdw/cc}$ with λ for $Et_4C \rightarrow Me_4C$ transformation in (a) water, (b) MeOH, and (c) DMSO.

λ, shown in Figure 12, is qualitatively similar to that of the $C_2H_6 \rightarrow CH_4$ transformation. However, the similarity between the variation of $\Delta G_{vdw/cc}$ in MeOH and DMSO is much more striking in this case than in Figure 11. The final values of $\Delta G_{vdw/cc}$ are 1.89 and 1.38 kcal/mol in MeOH and DMSO, respectively. The corresponding total free energy differences are 1.90 and 1.29 kcal/mol. A similar behavior may also be noted in the variation of $\Delta G_{vdw/cc}$ with λ for transformation of $Et_4C \rightarrow Me_4C$ as shown in Figure 13. There is an overlap between the curves of $\Delta G_{vdw/cc}$ in MeOH and DMSO for this transformation. The final values of $\Delta G_{vdw/cc}$ are 1.66 and 1.84 kcal/mol, in MeOH and DMSO, respectively, and the corresponding total free energy differences are 1.71 and 1.85 kcal/mol.

Discussion

(a) Radial Distribution Functions. The intermolecular pair distances obtained from the peak positions of the various rdfs of liquid DMSO agree very well with the pair distances obtained from the analysis of the X-ray diffraction data.[18] Both the experimental and the simulation studies indicate that the intermolecular pair distances are not well-defined, and these pair distances are characterized by large distributions. However, the first peak in the rdf of the C–O pair, which is the shortest intermolecular pair distance, is sharper than the peaks for the other pairs. This observation supports the suggestion[38] that the DMSO molecules are linked through some weak hydrogen bonds between the O atom and the methyl hydrogens. This view is also supported by the X-ray diffraction results.[18] In earlier models[9,38] of liquid DMSO based on some of its physical properties, it was proposed that DMSO molecules are associated by several types of short range interactions. In particular, the model proposing S=O--S=O chains in liquid DMSO appears to be favored.[9,39] A later study based on the dielectric data of liquid DMSO challenged[40] the view that DMSO dipoles form a definite alignment in the liquid and supported the view that the molecular arrangement is dictated by strong but nonspecific dipole–dipole interaction between the DMSO molecules. The present study establishes the following three important aspects of molecular arrangement in liquid DMSO. (1) Specific CH_3–O interaction exists between the nearest neighbor DMSO molecules. This observation is also supported by the X-ray diffraction study. (2) The absence of any well-defined correlation for the intermolecular S–O pairs implies that no S=O--S=O chains are formed in the liquid state as proposed in some of these earlier models.[9,38] (3) Almost identical rdfs for the S–S and O–O pairs reflect the correlation between the S=O dipoles. The intermolecular S–S and O–O pair distances from these rdfs suggest that the S=O dipoles are aligned roughly in an antiparallel manner. A snap shot picture of 216 DMSO molecules shown in Figure 14 reveals such an arrangement of the S=O dipoles between two nearest neighbor DMSO molecules. However, the alignment of the dipoles is interfered by the methyl groups and their interaction with oxygens. Therefore, no long-range order in the alignment of S=O dipoles similar to that in crystalline DMSO[41] is observed. This is expected since long-range order is not observed in the liquid state. However, the appearance of a second peak in most of the rdfs suggests that the molecular arrangement in liquid DMSO is ordered to some extent even beyond the first coordination sphere. Further, our study reveals that a DMSO molecule is coordinated by about 12 other DMSO molecules.

Figure 14. Stereoplot of the configuration of 216 DMSO molecules at the end of the molecular dynamics run. Each DMSO molecule is represented by three bonds. The S–O bond is shorter than the two S–C bonds.

The rdfs of the pairs involving the Cl^- ion and the S, C, and O atoms of DMSO show that the C atoms of DMSO are closest to the Cl^- ion. The anion is coordinated by about 14 methyl groups and seven sulfur atoms, indicating that about seven DMSO molecules are surrounding the anion. No experimental data on the coordination numbers of anions in DMSO are available. Studies[42,43] on aqueous solutions of Cl^- indicate that these ions are coordinated by about 6–8 water molecules. A gas-phase ab initio study[44] of the association of a single DMSO molecule with a Cl^- atom indicated that the anion lines up with the S=O bond dipole axis at a distance of 3.35 Å from the S atom. However, the present results suggest that the Cl^- ion is placed symmetrically closer to the two methyl groups, and the orientation of DMSO molecules around the anion is dictated by the Cl^-–CH_3 interaction rather than the Cl^-–S interaction. Moreover, the coordination sphere of S atom around the anion is irregular and the Cl^-–S pair distances spread from 4.25 to 5.35 Å. This is obviously due to the methyl groups hindering the approach of the anion towards the S atom.

The rdfs of the pairs involving Na^+ and the atoms of DMSO show that the Na^+–O peak is intense and sharp. As expected, the cation is closest to the O atom of DMSO. Since the O atom is at the negative end of the S=O dipole and can be approached by a positively charged ion unhindered, a well-defined coordination of O atoms around a cation is possible. The integration of the Na^+–O peak indicates that an exact number of five oxygens coordinate around the Na^+ ion. The coordination number for S around Na^+ ion is also 5. Hence, it is clear that the Na^+ ion is coordinated by five DMSO molecules. The Na^+–O pair peak is at 2.15 Å, and the Na^+–S pair peak is at 3.45 Å. The latter distance is close to the sum of the Na^+–O pair distance and the S=O bond distance (1.48 Å), suggesting that the cation almost lines up along the S=O dipole axis. This is consistent with the ab initio results of Magnera et al.[44] The Na^+–O distance of 2.15 Å in DMSO is smaller than the values (around 2.35 Å) observed

---

(38) Martin, D.; Weise, A.; Niclas, H. J. *Angew. Chem., Int. Ed. Engl.* **1967**, *6*, 318.

(39) Sen, U. *J. Am. Chem. Soc.* **1980**, *102*, 2181.

(40) Amey, R. L. *J. Phys. Chem.* **1968**, *72*, 3358.

(41) Thomas, R.; Schoemaker, C. B.; Eriks, K. *Acta Crystallogr.* **1966**, *21*, 12.

(42) (a) Palinkas, G.; Reide, W. O.; Heizinger, K. *Z. Naturforsch.* **1977**, *32A*, 1137. (b) Palinkas, G.; Ransai, T.; Hadzu, F. *Z. Naturforsch.* **1980**, *35A*, 107.

(43) Mezei, M.; Beveridge, D. L. *J. Chem. Phys* **1981**, *74*, 6902.

(44) Magnera, T. F.; Caldwell, G.; Sunner, J.; Ikuta, S.; Kebarle, P. *J. Am. Chem. Soc.* **1984**, *106*, 6140.

for this pair distance in aqueous and methanolic solutions.[11] However, a shorter distance between a cation and the oxygen atom of DMSO is expected due to the large dipole moment of DMSO. In fact, the K^+–O distance[44] in DMSO is shorter by about 0.25 Å than the same distance[43] in water.

(b) Free Energy Differences. The calculated free energy difference for $Cl^- \rightarrow Br^-$ transformation in water agrees well with the experimental value given by Friedman and Krishnan.[35] The agreement is not as good if the experimental values compiled by Marcus[45] are considered. The free energy difference for $Cl^- \rightarrow Br^-$ transformation reported by Friedman and Krishnan is 3.3 kcal/mol, while the value reported by Marcus is 6.2 kcal/mol. Lybrand et al.[34] calibrated the van der Waals parameters of the halogen ions based on the experimental results reported by Friedman and Krishnan. We have used the same parameters in our simulations. It is possible to reclibrate the van der Waals parameters based on the experimental values reported by Marcus and repeat the calculations on this transformation in the three solvents. However, we are confident that the qualitative differences in the patterns of ΔG variation for this mutation in the three solvents described here will not be much different from those obtained for the calculations with the recalibrated parameters. The free energy difference for this transformation in MeOH is in good agreement with the experimental value. However, the value for this transformation in DMSO is slightly overestimated. The reason for this overestimation may be due to the use of united atom model for DMSO. In this model, the positive charge on the methyl group is larger than that on the sulfur of DMSO (Table II), which makes the interaction between the Cl^- and the methyl groups more favorable than what is expected in an all atom model. In an all-atom representation of DMSO, the hydrogens of the methyl groups carry much smaller partial charges and hence interact less strongly with an anion. Therefore, the present transformation with an all-atom model of DMSO is expected to give a smaller free energy value closer to the experimental value. However, calculations involving an all-atom model will be more expensive computationally, since it makes the model of DMSO molecule bigger by six atoms. We must also point out that the error in the calculated free energy differences due to the use of a united atom model of DMSO is significant for the transformations involving anions only, and it is almost negligible for the other transformations discussed later. Even in the present case, the agreement between the calculated and experimental values is reasonable. Further, the present calculations correctly show the trend in the free energy differences of this transformation in the three solvents. This trend is depicted clearly in Figure 7, which shows that the rate of increase in $\Delta G_{vdw/cc}$ increases as one goes from DMSO through MeOH to water. The smaller decrease in free energy of solvation with an increase in ionic size is considered[44] to be the principal reason for the enhanced rates of bimolecular S_N2 reactions in dipolar aprotic solvents. On the basis of the analysis of the gas-phase equilibria of anions with DMSO, Magnera et al.[44] suggested that the lesser sensitivity of free energy of solvation to change in anion size is due to the larger radius of the inner shell of DMSO and its unfavorable orientation around anion. According to these authors, the larger inner shell radius makes solvation beyond the first shell insignificant, whereas it is significant for water. However, computer simulation studies[11,12,46] on aqueous and nonaqueous solutions show that the influence of ions beyond the first solvation shell is not significant in any of these solvents. It is interesting to note that a recent study[8] using a modified Born model for ionic solvation in nonaqueous solvents proposes different values for the cavity size of an ion in different solvents for accurate calculation of the heats of solvation. A later study from this group shows[47] that the larger association constant for an ion pair in a nonassociated solvent than in an associated solvent with the same dielectric constant can be due to larger cavity radii in nonassociated solvents. It is, therefore, very clear that the large ion–solvent distance in DMSO is an important factor that contributes to the smaller value of the ion–solvent interaction energy in DMSO as compared to that in water or MeOH. Nevertheless, the absence of any specific hydrogen bond interaction of Cl^- in DMSO has also some contribution to the difference in the interaction energies of this ion in DMSO and in the protic solvents, since Cl^- ion is known to be a hydrogen bond acceptor[5,16,46] in protic solvents. Therefore, the increasing size of the ion causes larger change in interaction energy in water and MeOH than in DMSO, and the same trend is reflected in the free energy differences as well. Though the calculated interaction energies of anions decrease as one goes from water through MeOH to DMSO, the trend in the interaction energy differences between the two anions in the three solvents is not clear, due to large fluctuations in these energies.

For transformation of $Na^+ \rightarrow K^+$, a good agreement is observed between the experimental and the calculated free energy differences in all the three solvents. The agreement between these values in water is encouraging, particularly because a recent free energy calculation using Monte Carlo simulation method by Migliore et al.[48] reported, for the same transformation, a value of 34.7 kcal/mol that is much larger than the experimental value of 17.5 kcal/mol. In two other recent studies[49,50] related to the ion recognition by different crown ethers in MeOH, the free energy difference for this transformation in MeOH is calculated to be between 19.2 and 21.7 kcal/mol. These values compare well with the value obtained in the present study and the experimental value of 17.8 kcal/mol. The excellent agreement between the calculated and experimental values for this transformation in DMSO is encouraging in view of the modest agreement observed for the previous transformation involving anions. Obviously, the use of a united atom model for DMSO has introduced negligible error in the calculated free energy differences for this transformation. The variation of $\Delta G_{vdw/cc}$ with λ shows that free energy of solvation for these ions is affected by the size of the solute ion to almost the same extent in all the three solvents. This is in contrast to the behavior of anions, in which case the sensitivity of free energy difference to the ionic size is different in different solvents. For cations, however, the most dominant solute–solvent interaction is the ion–dipole interaction. This interaction is equally strong in all the three solvents, since the cation can approach the negative charge center of the solvent molecules without any hindrance.[9] The rdf of Na^+–O in DMSO (Figure 4) shows a sharp peak at 2.15 Å and a well-defined coordination number of 5.0. Though the coordination number of Na^+ ion in DMSO is smaller than in water or MeOH, the ion–solvent interaction in DMSO is strong due to its large dipole. Therefore, the calculated interaction energies are almost equal for these ions in all the three solvents. Further, the differences between the interaction energies between the two cations in the three solvents are equally large (about 25 ± 10 kcal/mol). Hence, we observe almost equal free energy differences between the two cations in these solvents.

For the $Me_4N^+ \rightarrow NH_4^+$ transformation, the calculated free energy difference is almost the same (about −30 kcal/mol) in all three solvents. These values in water and MeOH are in good agreement with the experimental values. The experimental value for free energy of solvation of NH_4^+ in DMSO is not available for comparison. For this transformation, $\Delta G_{vdw/cc}$ decreases continuously with λ (Figure 9) at almost the same rate in the three solvents. This behavior is similar to that observed for $Na^+ \rightarrow K^+$ transformation. Though this result is surprising, it is consistent with the calculated interaction energies of these ions in the three solvents. The interaction energies of Me_4N^+ ion in the three solvents is almost the same, whereas the interaction energy of NH_4^+ ion is larger in DMSO than in water and MeOH. The

---

(45) Marcus, Y. *Ion Solvation*; John Wiley & Sons: New York, 1985; p 108.

(46) Chandrasekhar, J.; Spellmeyer, D. C.; Jorgensen, W. L. *J. Am. Chem. Soc.* **1984**, *106*, 903.

(47) Rashin, A. A. *J. Phys. Chem.* **1989**, *93*, 4664.

(48) Migliore, M.; Corongiu, G.; Clementi, E.; Lie, G. C. *J. Chem. Phys.* **1988**, *88*, 7766.

(49) Mazor, M. H.; McCammon, J. A.; Lybrand, T. P. *J. Am. Chem. Soc.* **1989**, *111*, 55.

(50) Grootenhuis, P. D. J.; Kollman, P. A. *J. Am. Chem. Soc.* **1989**, *111*, 2152.

larger interaction energy of NH_4^+ ion in DMSO is to be attributed again to the larger ion–dipole interaction. The continuous decrease in $\Delta G_{vdw/cc}$ observed for this transformation seems to result from large differences in interaction energies. The average difference between the interaction energies of the two ions in the three solvents is about 50 ± 10 kcal/mol. It appears, therefore, that these two ions are solvated in the three solvents in almost the same manner, and no special structure is formed by the water shell around these ions. This is consistent with the fact that the Me_4N^+ and NH_4^+ ions are not structure-making ions.[19]

A better case for elucidating the difference in the solvation behavior of water and nonaqueous solvents is the $Et_4N^+ \rightarrow Me_4N^+$ transformation since the larger Et_4N^+ cation is known[19] to induce structural effects in water. For this transformation, the calculated free energy differences in all three solvents are in good agreement with the experimental values. In this case, $\Delta G_{vdw/cc}$ varies in a manner different from that for the previous transformation. An examination of Figure 10, in which the variation of $\Delta G_{vdw/cc}$ is plotted against λ, leads to the following two observations: (1) the free energy decreases initially at a greater rate than in the later part of the transformation for all three solvents and (2) the rate of decrease in free energy at higher values of λ is higher in water than in MeOH and DMSO. The behavior in water is explained in our earlier paper[2] by presuming that the water molecules around the solute are "repulsed" by the hydrophobic methyl groups and form a tight solvent cage around the solute in accordance with Frank and Evans' hypothesis.[20] Because of the presence of the unit positive charge on tetraalkylammonium ions, the solvent is strongly pulled toward the solute which results in configurations wherein the solute and the surrounding solvent are further pushed into the repulsive region of the solute–solvent interaction potential surface. Since the van der Waals interaction due to four methyl groups are made to disappear during the mutation, the repulsive solute–solvent interaction is relieved, and the tight water structure around the solute is loosened. As a result, the free energy decreases aided by both decrease in interaction energy and increase in entropy due to solvent reorganization. Although the change in the interaction energy for this transformation in the three solvents is almost the same (Table VI), the decrease in free energy with mutation in MeOH and DMSO is not as large as in water. Therefore, we suspect that the contribution due to the solvent structure is not significant in MeOH and DMSO. Similar differences between water and the other two solvents are also observed for transformations of neutral alkanes discussed below.

For $C_2H_6 \rightarrow CH_4$ transformation, the agreement between the calculated free energy differences and the experimental values is not so good as in earlier transformations. The free energy differences for this transformation in the three solvents are underestimated by about 0.6–0.8 kcal/mol. As explained in our earlier paper[2] the discrepancy between the calculated, and the experimental values may be due to small interaction energies of these molecules in the three solvents (Table VI) and due to the unsymmetric change in the shape of the solute molecule during mutation. For $Me_4C \rightarrow CH_4$ and $Et_4C \rightarrow Me_4C$ transformation, the experimental values are available for MeOH only, and the calculated values compare well with those experimental values. For all three transformations in this series, $\Delta G_{vdw/cc}$ in MeOH increases almost linearly, whereas it increases in a zigzag manner in DMSO. In water, $\Delta G_{vdw/cc}$ initially decreases until λ is between 0.7 and 0.5, and then it increases. This difference in the variation of $\Delta G_{vdw/cc}$ between water and DMSO is interesting, considering that the calculated interaction energies are almost equal for these solutes in the two solvents (Table VI). The interaction energies of these solutes in MeOH are lower than those in water or DMSO. In each case, the interaction energy increases with decreasing size of the solute. Moreover, the change in interaction energy for the transformation of one alkane into another alkane is also the same in water and DMSO. If the enthalpic term has dominant contribution to free energy for the transformation in the two solvents, then the free energy should increase in both the cases. Such an increase is indeed observed in MeOH and DMSO. In contrast, the free energy initially decreases and then increases in water. This is obviously a result of reorganization of the tight water cage around these solutes. The absence of any such dip in the free energy variation in MeOH and DMSO suggests that these solvents do not form any tight solvent cage around apolar solutes. These observations support the view that the hydrophobic effect is a special property of water. For these transformations in DMSO, small dips are observed in the free energy variation curves at the beginning of the mutation. These dips may be caused by the statistical fluctuations in the calculated free energies or due to a structured solvent shell (similar to water shell but smaller in degree). Even if these small dips are taken as an indication of solvophobicity of DMSO toward apolar solutes, as is done in water, these dips are so small in comparison to the dips observed in water that the magnitude of this effect can only be insignificant in comparison to the effect observed in water.

Conclusions

Molecular dynamics simulations of liquid DMSO and its cationic and anionic solutions reported in the present study give important insights into the structure of liquid DMSO and its ionic solutions. These studies show that the molecular arrangement in liquid DMSO is dictated by specific short-range interaction between oxygen and methyl hydrogens and strong dipole–dipole interaction. Na^+ coordination in liquid DMSO is dictated by strong ion–dipole interaction, and a well-defined coordination sphere of five DMSO molecules is formed around this ion. Since the interaction of Cl^- ion with S=O dipole of DMSO is weakened by the intervening methyl groups, a well-defined coordination is not observed for this ion. However, our study reveals that the Cl^- ion is surrounded by about seven DMSO molecules in an irregular manner.

The calculated free energy differences for the transformations in water, MeOH, and DMSO are in good agreement with the experimental values. The nature of the solvent seems to have almost negligible influence on the variation of ΔG with the change in the solute size for positively charged alkali ions and smaller tetraalkylammonium ions. On the other hand, the ΔG of negatively charged halide ions are affected by the solute size to different extents in different solvents. The characteristic feature observed in the variation patterns of ΔG for alkanes and large tetraalkylammonium ions in water is not observed in MeOH or DMSO. Therefore, the present study supports the view that the hydrophobic effect is a peculiar property of water arising from the extensive hydrogen bonding between water molecules in the liquid state. We shall examine this subject further in our future studies in solvents forming an extensive hydrogen-bonding network.

Acknowledgment. All the calculations were performed on the CRAY X-MP/14SE supercomputer at the Research Institute of Scripps Clinic. We are grateful to Dr. Richard A. Lerner for providing the computer facilities and encouragement. This research is partially supported by a grant (R01-GM 39410) from the National Institute of Health. We are thankful to the reviewer for bringing refs 8 and 47 to our attention.